Image persistence and nonlinearity of intensified photodiode array detectors and their effect on CARS derived temperatures

Snelling, D.R.; Smallwood, G.J.; Sawchuck, R.A.

MARIA CLANCY
DGO
INST FOR CHEM PROCESS & ENVIR TECH
NATIONAL RESEARCH COUNCIL CANADA
M-12, ROOM 141, 1200 MONTREAL RD.
OTTAWA, ON K1A 0R6
CANADA

Title: **SPRING TECHNICAL MEETING OF THE CENTRAL STATES COMBUSTION INSTITUTE, DEARBORN, MI**

Author: SNELLING, D.R.; SMALLWOOD, G.J.; SAWCHUK, R.A.

Vol./Issue: APR

Date: 1989

Article Title: IMAGE PERSISTENCE AND NONLINEARITY OF INTENSIFIED PHOTODIODE ARRAY DETECTORS AND THEIR EFFECT ON CARS DERIVED TEMPERATURES

Image Persistence and Nonlinearity of Intensified Photodiode Array Detectors and their Effect on CARS Derived Temperatures

D.R. Snelling, G.J. Smallwood and R.A. Sawchuk

National Research Council of Canada
Ottawa, Ontario, Canada. K1A 0R6

Single-pulse, broadband coherent anti-Stokes Raman spectroscopy (CARS) has become an important diagnostic technique, particularly for combustion measurements of temperature and species concentration. The single pulse (10 ns) capability is crucial for the study of turbulent combustion, and in order to record a single pulse, the CARS radiation is dispersed and detected using an optical multichannel detector. We have investigated the image persistence and nonlinearity of these detectors and their effect on CARS derived temperatures.

The optical multichannel detectors (OMD) used for CARS spectroscopy are the intensified silicon intensified target (ISIT) vidicon and the intensified self-scanning silicon photodiode array (IPDA)[1]. The vidicons are widely recognized to suffer from an image persistence or lag problem but the IPDA is generally regarded as being free of image persistence[2] and has been used in CARS experiments with laser repetition rates up to 20 Hz.

During the course of an evaluation of a replacement IPDA detector we have investigated the image persistence problem and found it to be more pronounced than was commonly realised. We have measured the image persistence of a Tracor Northern TN-6132 IPDA and a Princeton Instruments IRY-1024 IPDA, both incorporating intensifiers (from two different manufacturers) using the standard P-20 phosphor.

The image persistence of the PI IRY-1024 is shown in Fig. 1 where the 10 Hz laser exposure was interrupted and the subsequent decay of the signal was followed. The read pattern (sequence of detector scans during 100 ms interval between laser pulses) of the detector is shown and all signals are expressed as a percentage of the last recorded laser pulse. The relative image persistence for the three detector scans in Fig. 1 is proportional to the integration times (time between individual diode reads) of 26.3 ms (READ #1), 46.5 ms (READ #2), 26.5 ms (READ #3). The image persistence can still be detected as much as 2.8 s following exposure and is 2.1% for read #1 in the first read cycle following the last exposure. (This represents the contribution of image persistence from previous exposures to CARS pulses). The image persistence is a function of the read pattern. Originally, for the TN-6132, we had selected a read pattern where the first read pulse following the exposure was delayed towards the end of the 100 ms exposure period to collect as much of the signal as possible and was followed by two "cleansing-scans" designed to remove any remaining signal from the detector. The second read pattern used, where read #1 was initiated 5 ms following the laser pulse, gave a much lower image persistence (0.57% compared to 1.5% for the first read pattern).

To understand the effect of the read pattern we have reconstructed the integrated IPDA intensity-plots. Between reads, which remove the accumulated charge on the diode array, the detector integrates the light from the image intensifier portion of the IPDA. Thus the signal is $\int_{T_1}^{T_2} I_p dt$

where T_1 and T_2 are the individual diode read times and I_p is the phosphor intensity. The integrated phosphor decay curves, which were constructed from data such as that in Fig. 1, following both an isolated exposure and the interruption of a continuous 10 Hz exposure, are shown in Fig. 2. The solid curves are directly calculated from experiment and the dotted curve was obtained by integrating the observed functional form of the phosphor decay at longer times ($I_p \propto t^{-n}$ where n is a constant) to infinity to obtain $\int_T^\infty I_p dt$ where T is the time of the last experimental observation. Thus the dotted curves include an estimate of the unobserved phosphor decay at time t greater than T (T=3 s).

From Fig. 2, it can be seen that there is an initial fast rise in the integrated phosphor intensity followed by a much slower build-up. In order to minimise the signal remaining from previous exposures while still collecting most of the current exposure, the total integration time between read #3 of the previous cycle and read #1 of the current cycle should be minimised, as in the read pattern for the PI IRY-1024 detector, shown in Fig. 1. In this way the image persistence has been reduced to approximately 0.5 and 2.0% for the TN-6132 and the PI IRY-1024, respectively.

We have attempted to evaluate the effect of this image persistence on CARS derived temperatures by synthesising purely theoretical spectra that are a mixture of two temperatures. This approximates a real CARS experiment where the image persistence includes diminishing effects from all the previous pulses. Six synthetic spectral libraries were created by adding 0.5% or 2.0% of 500 K, 700 K, or 1000 K theoretical CARS spectra to a standard library of spectra calculated (for a constant pressure of one atmosphere) at every 100 K from 300 K to 2100 K. The synthetic spectra were then treated as experimental spectra and fitted to the original library to obtain the best-fit temperatures. The error in best-fit temperatures that results from adding the image persistence of a cooler spectrum to a hot spectrum increases markedly with temperature (Fig. 3). This occurs because the CARS intensity decreases with increasing temperature (e.g. the peak intensity of a 2100 K spectrum is approximately 1/1000 that of a 300 K spectrum, assuming constant pressure). For the same reason the increase in best-fit temperature that results from adding the image persistence from a hot spectrum to a colder spectrum is negligible. The maximum increase in best-fit temperature observed was 3.3 K and for this reason this data was not presented in Fig. 3.

The temperature errors (Fig. 3) that result from the admixture of cold spectra are unacceptably large. In a turbulent flame with pockets of cool and hot gases, this would result in temperature histograms that were biased to lower temperatures where the biasing would depend on the particular time history as well as the temperature distribution. The fractional image persistence was found to increase with decreasing signal, making correction schemes difficult to implement.

The image persistence problem is clearly attributable to the phosphor, since the photocathode and microchannel plate intensifier have a fast response and since the diode array detector alone does not exhibit image persistence. It appears that the phosphor decay is complex and has a time constant that increases with time. In an attempt to avoid the problems associated with the P-20 phosphor we have evaluated a prototype Princeton Instruments IPDA with a faster rare earth phosphor, with the image persistence results shown in Fig. 4. The image persistence in the first

pulse (Read #1) following the last exposure is approximately 40 times less (at 0.06%) than for the corresponding detector with a P-20 phosphor (Fig. 1). The detector sensitivity was 4.5 photons/count (at 500 nm), which is comparable to the P-20 phosphor based detectors we have measured (1.7, 3.4, 2.9, 3.5 photons/count).

The P-20 phosphor based detectors examined exhibit a relative gain that falls off logarithmically with decreasing output signal (counts) as shown in Fig. 5. Correcting the experimental data for this nonlinearity results in best-fit temperatures between 40 K and 100 K greater at 1600 K. The prototype rare-earth phosphor did not exhibit any such nonlinearity thus suggesting that this too is associated with the P-20 phosphor.

There have been many comparisons of CARS derived temperatures with those obtained by techniques such as thermocouple and sodium line-reversal (Ref. 3 and 4 review earlier work). Recent comparisons[5,6,7], including our own[8], have claimed 1.0-1.5% accuracy and thus we were disconcerted to find this nonlinearity, which appears to be generic to P-20 based IPDA's, whose inclusion resulted in a substantial increase in best-fit temperatures.

We have considered whether stimulated Raman pumping of N_2 v=1 could be causing N_2 CARS flame spectra to appear anomalously hot and thus compensate for the neglect of detector nonlinearity. The room temperature N_2 CARS spectra frequently exhibit a small v=2→1 peak, evidence of stimulated Raman pumping of N_2 from level v=0 to v=1.

The CARS spectrometer, the generation of theoretical CARS spectra, and the data analysis procedures have been described previously[8]. The flame spectra were recorded in a H_2/air fueled flat-flame burner[8] whose temperature was independently measured to be 1577 $\pm$ 20 K.

In one series of experiments we deliberately defocussed the laser beams, producing a large increase in the stimulated Raman pumping of N_2 v=1, as shown by the experimental spectrum in Fig. 6. We characterise this pumping by measuring the ratio of the CARS v=2→v=1 peak amplitude (I_1) to the v=1→v=0 peak amplitude (I_0). We measure I_1 by determining its peak height above the tail of the fundamental band. For the room temperature N_2 spectrum in Fig. 6 the ratio I_1/I_0 = 0.019 whereas, before defocussing the laser beams, I_1/I_0 was typically 0.005.

An instrument function was obtained from the experimental spectrum in Fig. 6 by fitting it to synthetic CARS spectra that were calculated for a fixed rotational temperature of 294 K and varying vibrational temperature. A best-fit was obtained for a vibrational temperature (T_v) of 1325 K as shown in Fig. 6. The rotational relaxation times τ_R are sufficiently short (≈1.5 ns at room temperature and 4.5 ns at T=1600 K) compared to the laser pulse duration τ_L (τ_L ≈10 ns) to justify the implicit assumption of rotational relaxation. However, the vibrational relaxation times, even in the H_2/air flame, are very much longer than τ_L.

Synthetic CARS spectra convolved with this instrument function were used to fit the defocussed beam flame spectrum. The experimental spectrum (Fig. 7) is clearly vibrationally hotter and rotationally cooler than the best-fit theoretical spectrum (T=1775 K). A series of experiments with varying amounts of stimulated Raman pumping in the room temperature N_2 spectra was analysed and the results are shown in Fig. 8. A linear regression analysis of the data can be used to estimate the error in flame

spectrum temperature measurements if the I_1/I_0 ratio of the corresponding room temperature is known.

For data reported earlier[8], I_1/I_0 = 0.005 which would have meant that the best-fit flame spectra were ~45 K too high. This partially offsets the increase in best-fit temperature of 90 K that results from correcting this data for detector nonlinearity.

As a further demonstration of stimulated Raman pumping we have fitted experimental flame spectra to libraries of synthetic spectra with an augmented vibrational temperature. The resulting best-fit theory spectrum is shown in Fig. 9 where the vibrational temperature was 1881 K and the rotational/translational temperature was 1631 K. The augmented vibrational temperature clearly results in a much better fit as can be seen by comparing Fig. 9 with Fig. 7.

In summary, the image persistence of IPDA's incorporating P-20 phosphors is unacceptably large for 10 Hz single pulse CARS temperature measurements in turbulent combustion. A prototype IPDA incorporating a faster rare earth phosphor is shown to be more suitable. The P-20 based IPDA's are shown to exhibit a nonlinear response. Our previous omission in not correcting for detector nonlinearity and stimulated Raman pumping of N_2 v=1 had partially offsetting effects on CARS derived temperatures.

REFERENCES:

1. R.K. Chang and M.B. Long, "Optical Multichannel Detection," Appl. Phys. 50, 179 (1982).

2. Y. Talmi and R.W. Simpson, "Self-scanned Photodiode Array: A Multichannel Spectrometric Detector," Appl. Opt. 19, 1401 (1980).

3. M. Pealat, P. Bouchardy, M. Lefebvre and J.P. Taran, "Precision of Multiplex CARS Temperature Measurements," Appl. Opt. 24, 1012 (1985).

4. A.C. Eckbreth, "Laser Diagnostics for Combustion Temperature and Species," Abacus Press, Cambridge, Mass., U.S.A. (1988).

5. D.A. Greenhalgh, "CARS Thermometry for Low and High Pressure Combustion Systems," in proceedings of sixty-seventh AGARD conference (No. 399) on Advanced Instrumentation for Aero Engine Components held in Philadelphia (May 1986).

6. D.A. Greenhalgh and F.M. Porter, "CARS Application in Chemical Reactors, Combustion and Heat Transfer," in Proceedings, First International Laser Science Conference, Dallas (Nov. 1985).

7. F.Y. Yueh and E.J. Beiting, "Simultaneous N_2, CO, and H_2 Multiplex CARS Measurements in Combustion Environments using a Single Dye Laser," Appl. Opt. 27, 3233 (1988).

8. D.R. Snelling, G.J. Smallwood, R.A. Sawchuk and T. Parameswaran, "Precision of Multiplex CARS Temperatures using both Single-mode and Multimode Pump Lasers," Appl. Optics 26, 99 (1987).

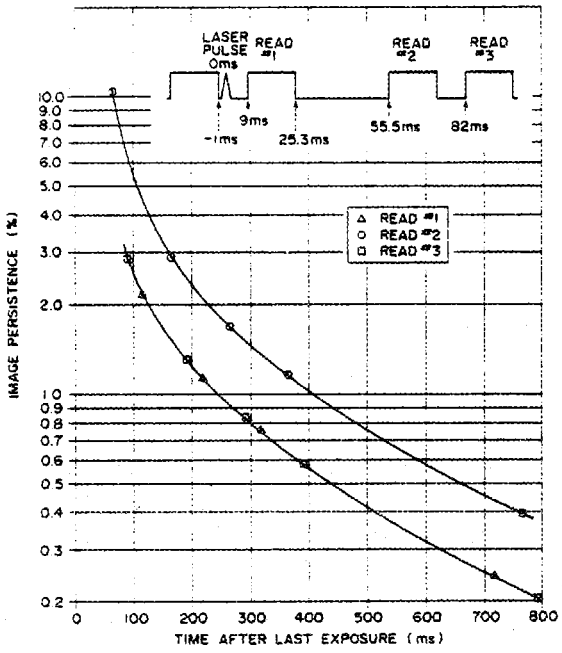

Fig. 1. Image persistence for a Princeton Instruments model IRY-1024 IPDA following an interrupted 10 Hz laser exposure.

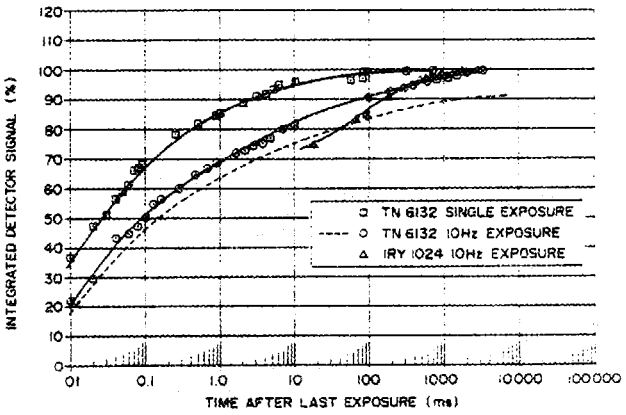

Fig. 2. Integrated phosphor intensities for interrupted 10 Hz and single laser exposures.

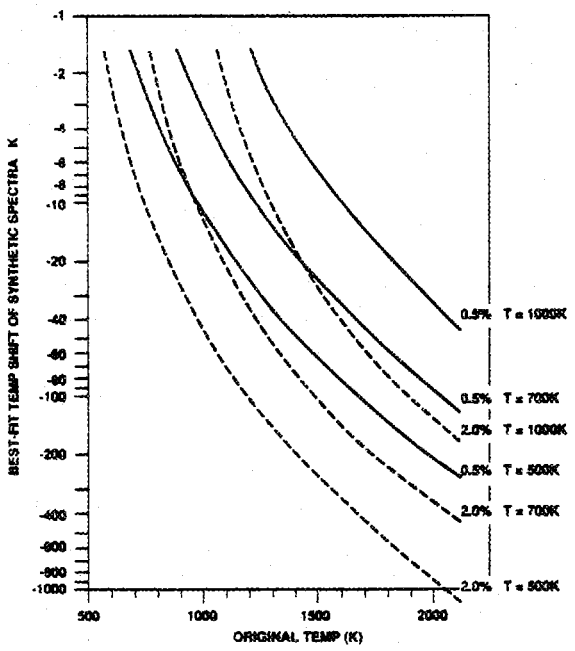

Fig. 3. Simulation of the effect of image persistence on best-fit CARS temperatures.

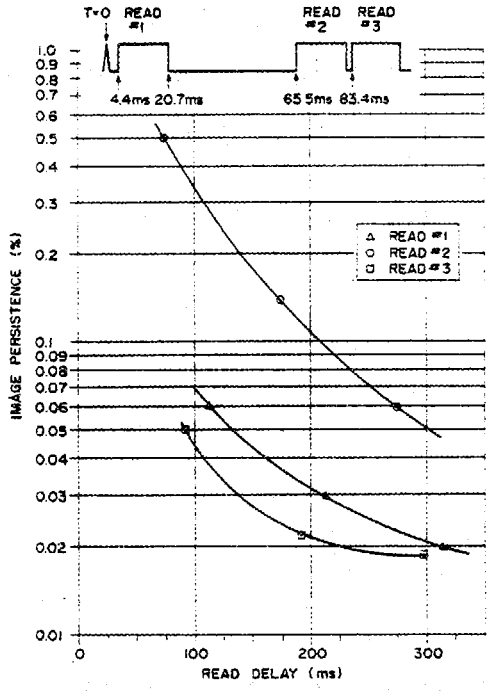

Fig. 4. Image persistence of a prototype Princeton Instruments detector with a faster rare-earth phosphor.

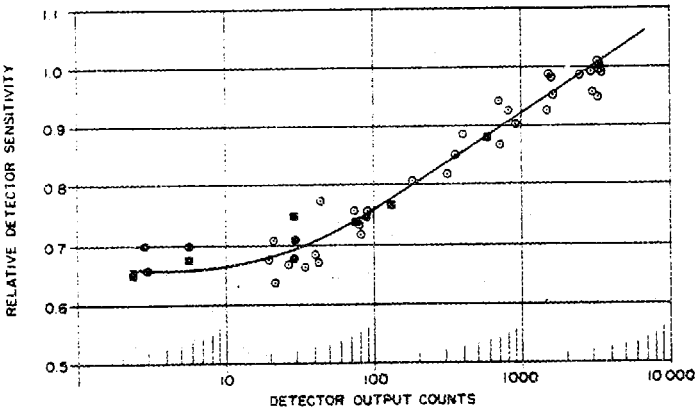

Fig. 5. Relative sensitivity of a Tracor Northern model TN-6132 IPDA detector.

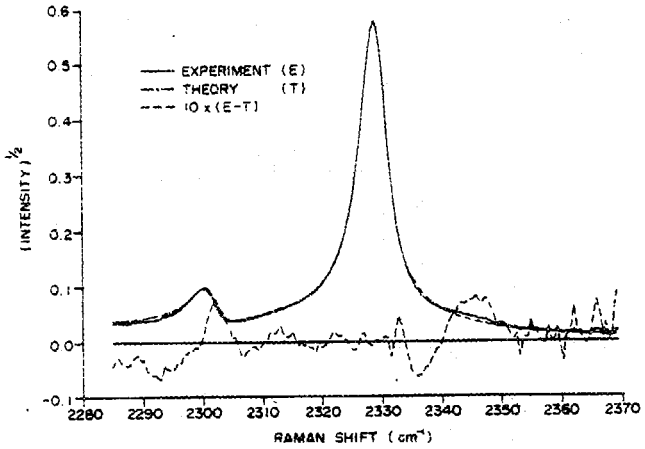

Fig. 6. Comparison of an experimental room temperature CARS spectrum to a theoretical N_2 CARS spectrum calculated for T_V=1325 K and T_R=294 K and convolved with a best-fit 6 parameter instrument function.

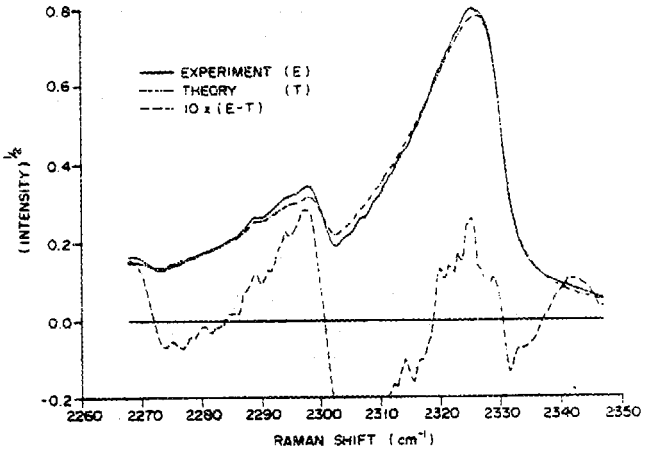

Fig. 7. Comparison of an experimental CARS flame spectrum to a best-fit theoretical spectrum (T=1775 K) convolved with an instrument function obtained from fitting a room temperature N_2 CARS spectrum.

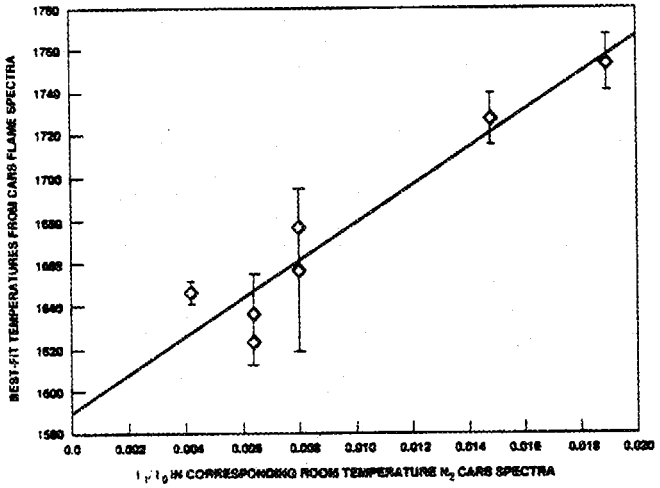

Fig. 8. Best-fit temperature for N_2 CARS flame spectra versus observed stimulated Raman pumping of N_2 v=1 in corresponding room temperature N_2 CARS spectrum.

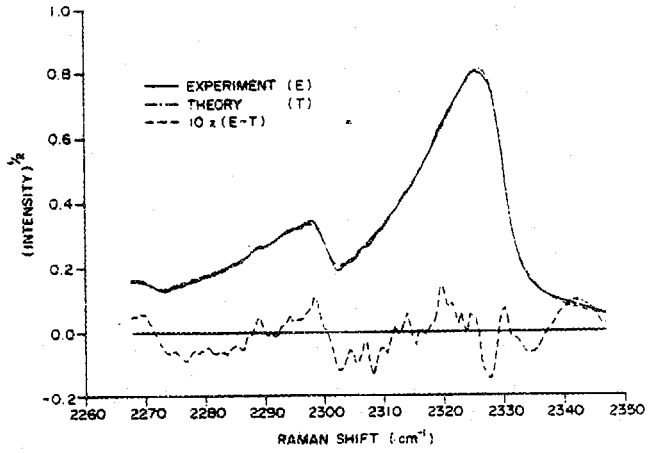

Fig. 9. Comparison of an experimental CARS flame spectrum to a best-fit theoretical spectrum (T_V=1881 K; T_R=1631 K) convolved with an instrument function obtained from fitting a room temperature N_2 CARS spectrum.